J Electr Eng Technol.2015; 10(2): 504-510
http://dx.doi.org/10.5370/JEET.2015.10.2.504

ISSN(Print) 1975-0102
ISSN(Online) 2093-7423

# Hierarchical Voltage Control of a Wind Power Plant Using the Adaptive $I_Q$-V Characteristic of a Doubly-Fed Induction Generator

**Jinho Kim*, Geon Park*, Jul-Ki Seok**, Byongjun Lee*** and Yong Cheol Kang†**

**Abstract** – Because wind generators (WGs) in a wind power plant (WPP) produce different active powers due to wake effects, the reactive power capability of each WG is different. This paper proposes a hierarchical voltage control scheme for a WPP that uses a WPP controller and WG controller. In the proposed scheme, the WPP controller determines a voltage error signal by using a PI controller and sends it to a doubly-fed induction generator (DFIG). Based on the reactive current-voltage ($I_Q$-V) characteristic of a DFIG, the DFIG injects an appropriate reactive power corresponding to the voltage error signal. To enhance the voltage recovery capability, the gains of the $I_Q$-V characteristic of a DFIG are modified depending on its reactive current capability so that a DFIG with greater reactive current capability may inject more reactive power. The proposed scheme enables the WPP to recover the voltage at the point of common coupling (PCC) to the nominal value within a short time after a disturbance by using the adaptive $I_Q$-V characteristics of a DFIG. The performance of the proposed scheme was investigated for a 100 MW WPP consisting of 20 units of 5 MW DFIGs for small and larger disturbances. The results show the proposed scheme successfully recovers the PCC voltage within a short time after a disturbance.

**Keywords:** Hierarchical voltage control, DFIG, Wake effect, Reactive current capability

## 1. Introduction

The voltages at all buses in a power grid should be maintained within a specified operational range to ensure stable operation. The voltage at a node, which is called as a local variable, should be controlled by a generator or the reactive power compensating unit closest to the applicable node. In the case of a grid with high wind penetration, WGs and WPPs should be capable of supporting the voltage at the PCC when a disturbance occurs. To achieve this function, a WPP should not only ride through the fault, but also supply the reactive power during the fault and after the fault clearance [1-3]. Therefore, a hierarchical voltage control that combines WPP and WG controllers is essential to manage the collective response of the WGs in a WPP.

Various research reports have dealt with hierarchical control schemes of DFIG-based WPPs for voltage stability [407]. Required reactive power is dispatched to DFIGs by considering the reactive power capability of each DFIG [4, 5]. To ensure that the injected reactive power at a PCC matches the reactive power setpoint given by a WPP controller, the setpoint is distributed to the DFIGs in a WPP and the DFIGs are operated in a reactive power control mode. The required reactive power at a certain node is met by the reactive power setpoint distributed to each DFIG. However, the voltage recovery is slow because the DFIG controller needs a command signal from the WPP controller to react to a sudden voltage change.

A centralized voltage control for a WPP has been proposed in which the required reactive current is allocated to a DFIG by using a weighting factor that is inversely proportional to the active power output of each DFIG [6]. In this scheme, each DFIG injects a different reactive power depending on the operating condition. However, this scheme is unable to react immediately after a disturbance due to the reactive current control mode of the DFIG.

A hierarchical reactive power control scheme for WPPs has been suggested for fast voltage support [7]. In this scheme, a DFIG operates in a voltage control mode by using the fixed $I_Q$-V relationship to react quickly against voltage changes. A WPP controller determines the required reactive power based on the reactive power to voltage (Q-V) requirement specified in the UK Grid Code. This is then converted into the voltage setpoint to be sent to a DFIG. This scheme showed good performance in terms of fast voltage support when a large voltage dip occurs. However, for small disturbances, steady-state errors are inevitable due to the small gain in the Q-V characteristic of the WPP controller.

This paper proposes a hierarchical voltage control scheme for a DFIG-based WPP that uses the adaptive $I_Q$-V

† Corresponding Author: Dept. of Electrical Engineering, WeGAT Research Center, and Smart Grid Research Center, Chonbuk National University, Korea. (yckang@jbnu.ac.kr)
* Dept. of Electrical Engineering and WeGAT Research Center, Chonbuk National University, Korea. ({jkim, powerupme}@jbnu.ac.kr)
** Dept. of Electrical Engineering, Yeungnam University, Korea. (doljk@ynu.ac.kr)
*** Dept. of Electrical Engineering, Korea University, Korea. (leeb@korea.ac.kr)
Received: October 14, 2014; Accepted: October 27, 2014

characteristic of a DFIG. In the proposed scheme, a WPP controller generates a voltage error signal by using a PI controller and sends it to a DFIG. The DFIG responds to the voltage error signal by injecting reactive power based on its $I_Q$-V characteristic. To enhance the voltage recovery capability, the gains of the $I_Q$-V characteristic of a DFIG are modified depending on its reactive current capability so that a DFIG with greater reactive current capability may inject more reactive power. The performance of the proposed scheme was investigated for a 100 MW WPP consisting of 20 units of 5 MW DFIGs for various disturbances by using an EMTP-RV simulator.

## 2. Hierarchical Voltage Control Scheme of a WPP using the Adaptive $I_Q$-V Characteristic of a DFIG

### 2.1 Control strategies of a DFIG

Fig. 1 shows a typical configuration of a DFIG. The rotor-side converter (RSC) illustrated schematically in Fig. 2 controls the active and reactive powers of a stator winding. To maximize the stator active power, herein the active power reference, $P_{ref}$, is set as follows [9]:

$$P_{ref} = k_g \omega_r^3 \tag{1}$$

where $k_g$ is a function of parameters such as the gear-ratio, blade length, and blade profile, and $\omega_r$ is the rotor speed.

In addition, a voltage control function is implemented in the RSC controller to keep the stator terminal voltage at a nominal value.

On the other hand, the grid-side converter (GSC) illustrated schematically in Fig. 3 can control the dc-link voltage to be constant and inject the reactive power from

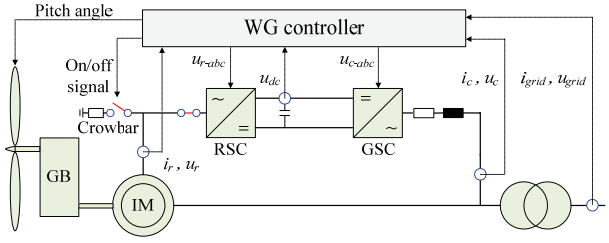


**Fig. 1.** Typical configuration of a DFIG

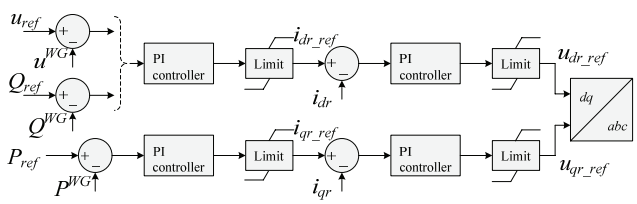


**Fig. 2.** RSC control scheme

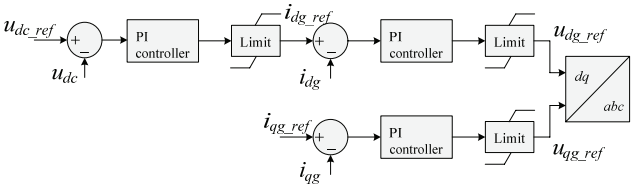


**Fig. 3.** GSC control scheme

the GSC to support the grid voltage. In the proposed design, the GSC maintains only the dc-link voltage as a constant without any reactive power injection.

### 2.2 Conventional control schemes [6, 7]

Fig. 4 schematically illustrates the WPP and WG controllers of a conventional voltage control scheme [6]. The WPP controller calculates the required reactive currents, $i_{dr\_ref}$ and $i_{qg\_ref}$, from the voltage error by means of a PI controller, and the reactive current setpoints for a DFIG, $i^{WGi}_{dr\_ref}$ and $i^{WGi}_{qg\_ref}$, respectively, are determined by:

$$i^{WGi}_{dr\_ref} = \frac{1}{K_i} i_{dr\_ref}$$
$$i^{WGi}_{qg\_ref} = \frac{1}{K_i} i_{qg\_ref} \tag{2}$$

$$K_i = \frac{P^{WGi}}{P_{avg}} \tag{3}$$

where $P_{avg}$ is the average active power for all WGs and

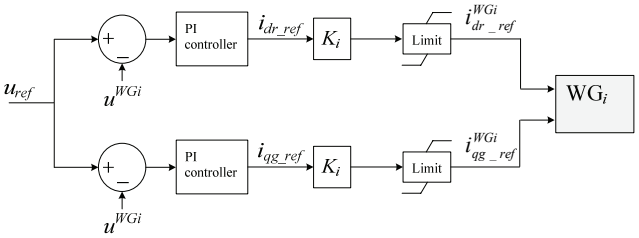


(a) WPP controller

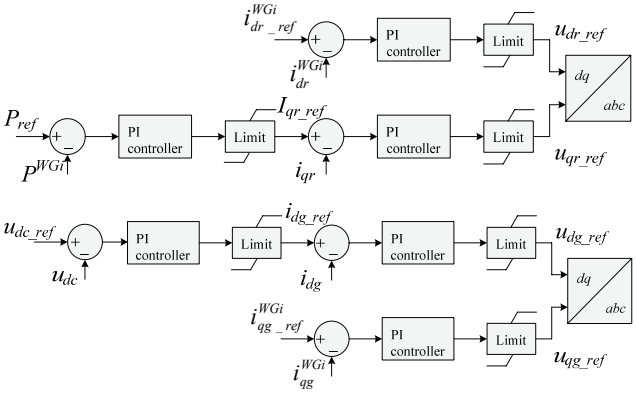


(b) WG controller

**Fig. 4.** Conventional voltage control scheme [6]

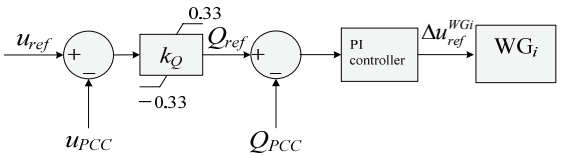


(a) WPP controller

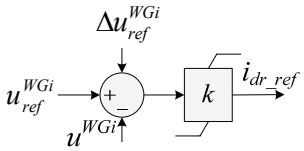


(b) WG controller

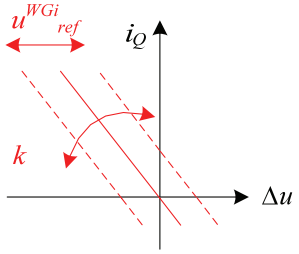


($\Delta u = \Delta u^{WGi}_{ref} + u^{WGi}_{ref} - u^{WGi}$)

(c) $I_Q$-V characteristic of a DFIG in [7]

**Fig. 5.** Conventional reactive power control scheme [7]

$P^{WGi}$ is the active power output of $WG_i$.

The reactive power allocation is inversely proportional to the active power output of a WG, because a WG supplying less active power can supply more reactive power. This control scheme allows a WPP to supply much reactive power from a DFIG. However, the scheme is unable to react to a voltage dip immediately after a disturbance due to the reactive current control mode used for the DFIG controllers.

Fig. 5 shows a conventional reactive power control scheme for a WPP [7]. The WPP controller generates the reference voltage signal, $\Delta u^{WGi}_{ref}$, which is determined from the required Q-V characteristic for a WPP specified in the British Grid Code [8] (see Fig. 6) by using a PI controller. The Q-V characteristic gain, $k_Q$, is set to:

$$k_Q = \frac{Q_{\max} - Q_{\min}}{0.1} \tag{4}$$

where $Q_{max}$ and $Q_{min}$ are the maximum and minimum reactive power of a WPP and are set to 33% of the rated power of the WPP. In the Fig. 5(a) scheme, $k_Q$ is set to 6.6. Then, the reactive power setpoint, $Q_{ref}$, is compared to the reactive power measured at the PCC. From the reactive power error, $\Delta u^{WGi}_{ref}$ is obtained by using a PI controller and sent to $WG_i$.

The DFIGs in the WPP operating in a voltage control mode generate the reactive current reference, $I_{dr\_ref}$, by using the $I_Q$-V characteristic (see Fig. 5(c)) gain, $k$. All

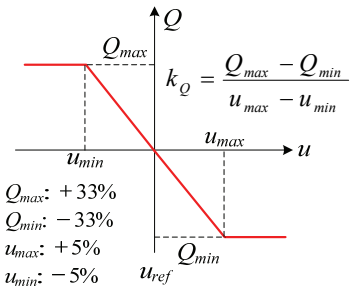


**Fig. 6.** Q-V characteristic of the UK grid code [9]

DFIGs have the same gain. Input signals of the WG controller consist of the voltage reference, $u^{WGi}_{ref}$, for $WG_i$, the measured voltage of the WG terminal, $u^{WGi}$, and $\Delta u^{WGi}_{ref}$. The values of $k$ and $u^{WGi}_{ref}$ are set to 2 and 1 pu, respectively. Note that the conventional scheme in [7] uses a fixed $k$ over the entire range of operating conditions for a DFIG.

This control scheme shows good performance in terms of fast voltage support when a large voltage dip occurs. However, for a small disturbance, steady-state errors are inevitable due to the small gain of the Q-V characteristic of the WPP controller.

### 2.3 Proposed voltage control scheme

Fig. 7 shows the WPP and WG controllers of the proposed hierarchical voltage control scheme. The active power output of a WG in a WPP depends on the wind speed arriving at that WG. Thus, WGs generate different active powers and the reactive power capabilities differ among WGs [10, 11]. To enhance the voltage support capability of a WPP after a disturbance, the proposed control scheme lets the WG generating less active power output supply more reactive power.

To maintain the PCC voltage as a voltage setpoint, the WPP controller operating in the voltage control mode generates $\Delta u^{WGi}_{ref}$ by using a PI controller, and then sends it to $WG_i$, which is operating in the voltage control mode as in [7].

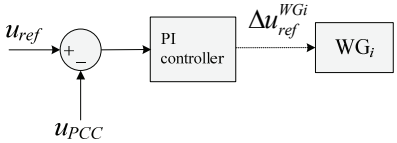


(a) WPP controller

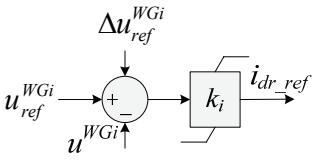


(b) WG controller

**Fig. 7.** Proposed hierarchical voltage control scheme

The WG controller of the proposed scheme has the same $I_Q$-V characteristic as that of [7], but modifies the $I_Q$-V gain $k_i$ depending on the reactive current capability, as shown in Fig. 8. This enables the DFIGs with high reactive current capabilities to inject more reactive power.

Based on the reactive current capability of a DFIG, $k_i$ is calculated by:

$$k_i = \frac{I_{Q\_\max}^{WGi} - I_{Q\_\min}^{WGi}}{\Delta u} \tag{5}$$

where $I^{WGi}{}_{Q\_max}$ and $I^{WGi}{}_{Q\_min}$ are the maximum and minimum reactive currents of a $WG_i$. In addition, $\Delta u$, which is the bandwidth of the $I_Q$-V characteristic, is set to 0.2 pu.

Fig. 8 shows the reactive current capability curve of the DFIG. The $I^{WGi}{}_{Q\_max}$ and $I^{WGi}{}_{Q\_min}$ in (5) are obtained from the reactive current capability curve of a DFIG (see Fig. 8) at an active power output.

Fig. 9 shows examples of the $I_Q$-V characteristics of DFIGs. The black, red, and blue lines represent the $I_Q$-V characteristics of $WG_1$, $WG_2$, and $WG_3$, respectively. The active currents of $WG_1$, $WG_2$, and $WG_3$ are assumed to be 0.80, 0.60, and 0.50 pu, respectively. The ranges of the reactive current of $WG_1$, $WG_2$, and $WG_3$ are (–0.60 pu, 0.60 pu), (–0.80 pu, 0.80 pu), and (–0.87 pu, 0.87 pu), respectively. Thus, $k_1$, $k_2$, and $k_3$ are set to 6.00, 8.00, and 8.70, respectively.

The proposed adaptive gain scheme allows WGs to inject the maximum reactive power of a WG for a voltage deviation larger than 0.1 pu, and to inject reactive power proportional to the maximum value in the linear region.

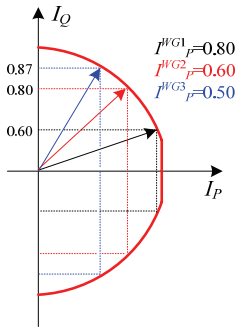


**Fig. 8.** Reactive current capability curve of a DFIG

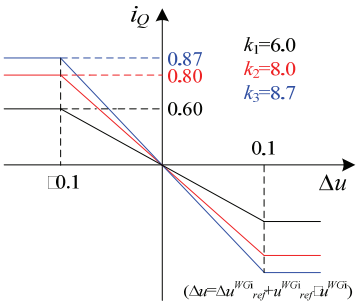


**Fig. 9.** Adaptive $I_Q$-V characteristic of a DFIG

## 3. Wake speed calculation

WGs in a WPP generate electricity by extracting the kinetic energy of the wind. Thus, upstream WGs reduce the wind speed arriving at WGs further downstream. This shadowing effect is called the wake effect. To calculate the wind speed at each WG, the method suggested in [12] is used to consider the cumulative impact of multiple shadowing and the effect of the wind direction. The resulting wind speed of a $WG_j$, $v_j$, can be obtained by:

$$v_j = v_{j0} - \sqrt{\sum_{\substack{i=1 \\ i \neq j}}^{n} \beta_i^2 \left(v_{wk}(x_{ij}) - v_{j0}\right)^2} \tag{6}$$

where $v_{j0}$ is the incoming wind speed at $WG_j$ without any shadowing, $x_{ij}$ is the radial distance between $WG_i$ and $WG_j$, $v_{wk}(x_{ij})$ is the speed of the wind approaching $WG_j$ from the shadowing $WG_i$, $\beta_i$ is the ratio of the area of $WG_j$ under the shadow of $WG_i$ to its total area, and $n$ is the total number of WGs.

## 4. Case studies

To investigate the performance of the proposed scheme, the model system illustrated schematically in Fig. 10 was chosen, which includes a WPP and the grid. This WPP consists of 20 units of 5 MW DFIGs. Four DFIGs are connected to each feeder through 2.3/33 kV transformers. Five collector feeders are connected to the 33/154 kV substation transformer through 33 kV submarine cables and then to the PCC through a 10-km-long 154 kV submarine cable. The distance between two neighboring

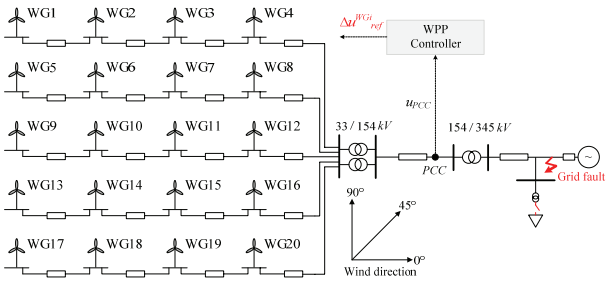


**Fig. 10.** Model system

**Table 1.** Wind speeds at all WGs in the WPP

| Free wind speed of 10 m/s at 90° | | | | Free wind speed of 12 m/s at 45° | | | |
|---|---|---|---|---|---|---|---|
| 6.90 | 6.90 | 6.90 | 6.90 | 12 | 11.79 | 11.06 | 10.38 |
| 7.63 | 7.63 | 7.63 | 7.63 | 12 | 11.79 | 11.06 | 10.38 |
| 8.43 | 8.43 | 8.43 | 8.43 | 12 | 11.79 | 11.06 | 11.06 |
| 9.32 | 9.32 | 9.32 | 9.32 | 12 | 11.79 | 11.79 | 11.79 |
| 10 | 10 | 10 | 10 | 12 | 12 | 12 | 12 |

DFIGs was set to 1 km. The short circuit capacity of the grid and the short circuit ratio of the WPP were set to 600 MVA and 5, respectively.

The proposed scheme was tested and compared with the conventional schemes [6] and [7] for two cases of wind speed and direction. The WPP controller sends a reference signal to the WG controller every 0.1 s. Table 1 shows the wind speeds for the two cases.

### 4.1 Case 1: 60 MVAr reactive load connection at 7 s with the free wind speed of 10 m/s at 90°

Fig. 11 shows the results for case 1. At 7 s, the inductive load of 60 MVAr is connected to a grid. The reactive power support of a WPP depends both on the command signal from the WPP controller and the control mode of the WG controller. However, because the command signal may not be delivered to the WG controller immediately after a load connection, the control mode of the WG controller is crucial. The proposed scheme and the conventional scheme in [7] supplied larger reactive powers than the conventional scheme in [6] (see Fig. 11(b)) because the WG controllers operated in the voltage control mode. In case 1, the proposed scheme modified $k_i$ depending on the available reactive power. The gains of $WG_1$, $WG_5$, $WG_9$, $WG_{13}$, and $WG_{17}$ on the first column were set to 9.71, 9.57, 9.34, 8.98, and 8.63, respectively. Thus, $WG_1$, which has the largest reactive current capability among the five DFIGs, injected the most reactive power into the grid (see Fig. 11(c)).

However, as mentioned in Subsection 2.2, after 7.21 s the conventional scheme in [6] supplies less reactive power than the other two schemes because the WPP controller of the conventional scheme in [7] generates a command signal with a small value, resulting from a small PCC voltage deviation. The results indicate that for a WPP controller, the voltage control mode shows a better performance than the reactive power control mode for the small voltage deviation.

### 4.2 Case 2: 0.6 pu voltage grid fault at 7 s with free wind speed of 12 m/s at 45°

Fig. 12 shows the results for case 2. At 7 s, a 0.6 pu grid fault occurs and lasts for 200 ms. From 7.0 s to 7.1 s, the proposed scheme and the conventional scheme in [7] injected greater reactive power than the conventional scheme in [6] as shown in Fig. 12(b). In addition, in case 2, the gains of $WG_1$, $WG_2$, $WG_3$, and $WG_4$ on the top row were set to 7.09, 7.32, 8.03, and 8.51, respectively. They injected different reactive powers based on the different gains. $WG_4$, which has the greatest reactive power capability among the four DFIGs, injected the most

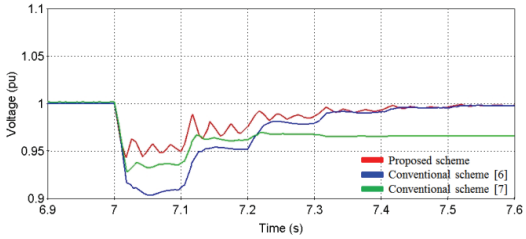


(a) PCC voltages

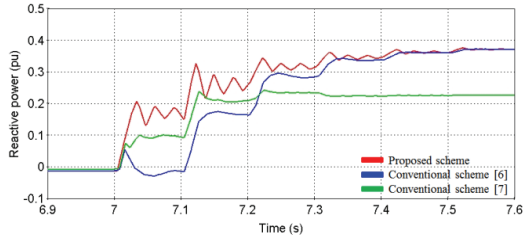


(b) PCC reactive power

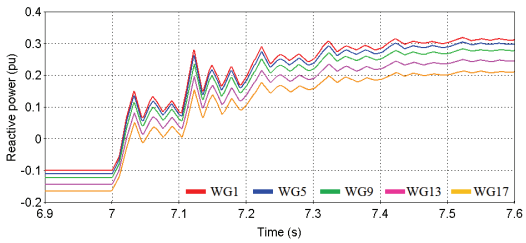


(c) Reactive power of $WG_1$, $WG_5$, $WG_9$, $WG_{13}$, and $WG_{17}$

**Fig. 11.** Results for case 1

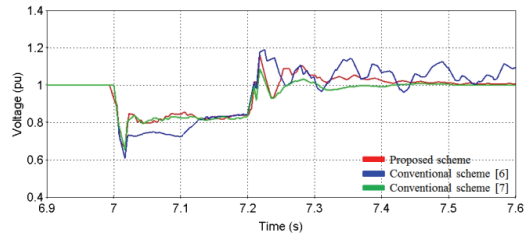


(a) PCC voltages

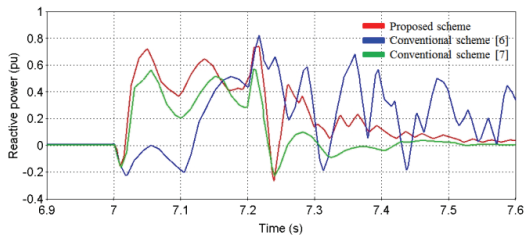


(b) PCC reactive power

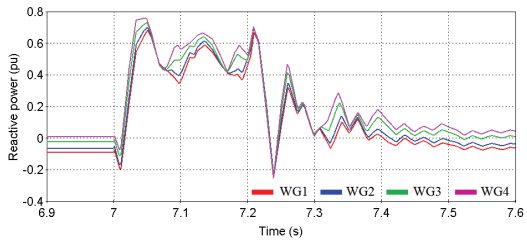


(c) Reactive power of $WG_1$, $WG_2$, $WG_3$, and $WG_4$

**Fig. 12.** Results for case 2

reactive power (see Fig. 12(c)). Note that $WG_1$ injected the least reactive power in case 2 whereas it injected the greatest reactive power in case 1. This is because the DFIGs in the proposed scheme modify their gains depending on the operating conditions. On the other hand, after the fault clearance, the reactive power for the conventional scheme in [6] fluctuated more severely than that in the other schemes because it uses weighting factors, which fluctuate due to the active power fluctuation caused by the voltage deviation.

Immediately after the fault, the PCC voltage increased from 0.6 pu to 0.8 pu for the proposed scheme and the conventional scheme in [7] because the they use the voltage control mode as a WG controller. After the fault clearance, the PCC voltage starts to increase and the WG controllers in the proposed scheme and the conventional scheme in [7] respond to the sudden voltage increase by reducing $i_{dr\_ref}$ (see Figs. 5(b) and 7(b)). On the other hand, as the conventional scheme in [6] must wait for the command signal from the WPP controller, the voltage is reduced more than in the other two schemes. Furthermore, the PCC voltage for the proposed scheme and the conventional scheme in [7] recovered to a nominal value within a short time, whereas in the conventional scheme in [6] it took more time to recover due to the weighting factors, which are inversely proportional to the active power output.

## 5. Conclusion

This paper proposes a hierarchical voltage control scheme for a DFIG-based WPP that uses the adaptive $I_Q$-V characteristics of DFIGs. In the proposed scheme, both WPP and WG controllers operate in the voltage control mode. The WPP controller determines the voltage error signal by using a PI controller and sends it to each DFIG. From the voltage error signal, the DFIGs supply the reactive power based on the adaptive $I_Q$-V characteristic gains, which depend on the available reactive current capabilities of the DFIG.

The test results demonstrate that the $I_Q$-V gains of DFIGs in the proposed scheme are modified depending on the operating conditions and thus the WPP successfully recovers the PCC voltage to its nominal value within a short time for the large and small disturbances.

## Acknowledgements

This work was partly supported by the National Research Foundation of Korea (NRF) grant funded by the Korea government (MSIP) (NO.2010-0028509) and partly by the National Research Foundation of Korea (NRF) grant funded by the Korea government (MEST) (NO.2011-0017650).

## References

[1] M. Tsili and S. Papathanassiou, "A review of grid code technical requirements for wind farms," *IET Renewable Power Generation*, vol. 3, no. 3, pp. 308-332., Sept. 2009.

[2] E.ON Netz GmbH, "Grid Code: High and Extra High Voltage", Aug. 2006.

[3] H. Geng, C. Liu, and G. Yang, "LVRT capability of DFIG-based WECS under asymmetrical grid fault condition", *IEEE Trans. on Industrial Electronics*, vol. 60, no. 6, pp. 2495-2509, Jun. 2013.

[4] A. Tapia, G. Tapia, and J. X. Ostolaza, "Reactive power control of wind farms for voltage control applications," *Renew. Energy*, vol. 29, no. 3, pp. 377-392, Mar. 2004.

[5] D. Hansen, P. Sorensen, F. Iov, and F. Blaabjerg, "Centralised power control of wind farm with doubly fed induction generators," *Renew. Energy*, vol. 31, no. 7, pp. 935-951, Jun. 2006.

[6] M. E. Moursi, G. Joos, and C. Abbey, "A secondary voltage control strategy for transmission level interconnection of wind generation," *IEEE Trans. on Power Electronics*, vol. 23, no. 3, pp. 1178-1190, May 2008.

[7] J. Fortmann and I. Erlich, "Use of a deadband in reactive power control requirements for wind turbines in European grid code", *11th international workshop on large-scale integration of wind power into power systems*, Lisbon, Portugal, 13-15 Nov. 2012.

[8] National Grid, "The Grid Code– Issue 4, Revision 5", 31st Dec. 2010.

[9] B. Shen, B. Mwinyiwiwa, Y. Zhang, and B. Ooi, "Sensorless Maximum Power Point Tracking of Wind by DFIG Using Rotor Position Phase Lock Loop," *IEEE Trans. on Power Electronics*, Vol. 24, No. 4, pp. 942-951, Apr. 2009.

[10] T. Lund, P. Sorensen, and J. Eek, "Reactive power capability of a wind turbine with doubly fed induction generator," *Wind energy*, vol. 10, pp. 379-394, Apr. 2007.

[11] S. N. Singh, J. Østergaard, and B. Singh, "Reactive power capability of unified DFIG for wind power generation," in *Proc. IEEE Power & Energy Society General Meeting*, Minneapolis, MN, USA, pp. 1-7, Jul. 2010.

[12] F. Koch, M. Gresch, F. Shewarega, I. Erlich, and U. Bachmann "Consideration of wind farm wake effect in power system dynamic simulation," *Power Tech*, Russia, Jun. 2005.

**Jinho Kim** received his B.S. degree from Chonbuk National University, Korea in 2013. He is currently pursuing his M. S. degree at Chonbuk National University. He is also an assistant researcher of the WeGAT Research Center supported by the Ministry of Science, ICT, and Future Planning (MSIP), Korea. His research interests include the development of control and protection methods for wind power plants.

**Geon Park** received his B.S. degree from Chonbuk National University, Korea in 2014. He is currently pursuing his M. S. degree at Chonbuk National University. He is also an assistant researcher of the WeGAT Research Center supported by the MSIP, Korea. His research interests include the development of fault ride-through scheme for offshore wind power plants.

**Jul-Ki Seok** received the B.S., M.S., and Ph.D. degrees from Seoul National University, Seoul, Korea, in 1992, 1994, and 1998, respectively, all in electrical engineering. From 1998 to 2001, he was a Senior Engineer with the Production Engineering Center, Samsung Electronics, Suwon, Korea. Since 2001, he has been a member of the faculty of the School of Electrical Engineering, Yeungnam University, Gyeongsan, Korea, where he is currently a Professor. His specific research areas are motor drives, power converter control of offshore wind farms, and nonlinear system identification related to the power electronics field.

**Byongjun Lee** received B.S. degree from Korea and Ph.D. degrees in Electrical Engineering from Iowa State University in 1991 and 1994 respectively. He is currently a professor in the Dept. of Electrical Engineering at Korea University. His interests include power system operation, voltage control, system protection schemes, PMU and large-scale wind farm integration.

**Yong Cheol Kang** received his B.S., M.S., and Ph.D. degrees from Seoul National University, Korea, in 1991, 1993, and 1997, respectively. He has been with Chonbuk National University, Korea, since 1999. He is currently a professor at Chonbuk National University, Korea, and the director of the WeGAT Research Center supported by the MSIP, Korea. His research interests include the development of new protection and control systems for wind power plants.